

# Energy density for chiral lattice fermions with chemical potential

Christof Gattringer<sup>a</sup> and Ludovit Liptak<sup>b</sup>

<sup>a</sup>*Institut für Physik, FB Theoretische Physik, Universität Graz,  
Universitätsplatz 5, 8010 Graz, Austria*

<sup>b</sup>*Institute of Physics, Slovak Academy of Sciences,  
Dúbravská cesta 9, 845 11 Bratislava 45, Slovak Republic*

We study a recently proposed formulation of overlap fermions at finite density. In particular we compute the energy density as a function of the chemical potential and the temperature. It is shown that overlap fermions with chemical potential reproduce the correct continuum behavior.

PACS numbers: 11.15.Ha, 12.38.Gc

## I. INTRODUCTION

Over the last two decades lattice gauge theory was turned into a powerful qualitative tool for analyzing QCD. This progress is in part due to the advances in algorithms and computer technology, but also on the conceptual side important breakthroughs were made. Most prominent among these is the correct implementation of chiral symmetry on the lattice based on the Ginsparg-Wilson equation for the Dirac operator [1].

An application of lattice techniques which has seen a lot of attention in recent years, is the study of QCD at finite temperature. The lattice implementation of the chemical potential  $\mu$ , necessary for such an analysis, is not straightforward, however. It is well known [2], that a naive introduction leads to  $\mu^2/a^2$  contributions which diverge in the continuum limit when the lattice spacing  $a$  is sent to zero. For more traditional formulations, such as the Wilson or staggered Dirac operators, the problem has been solved by introducing the chemical potential in the same way as the 4-component of the gauge field.

A satisfactory implementation of the chemical potential should be compatible with chiral symmetry on the lattice based on the Ginsparg-Wilson equation. When attempting to introduce the chemical potential into the only solution of the Ginsparg-Wilson equation known in closed form, the overlap operator [3], a potential problem quickly surfaces: defining the sign function of a non-hermitian matrix. In [4] Bloch and Wettig proposed a solution based on an analytic continuation of the sign function into the complex plane. It was shown, that the eigenvalue spectra of this construction match the expectations from random matrix theory.

In this letter we analyze the proposal [4] further and study the energy density of free, massless overlap fermions with chemical potential. The dependence of the energy density on  $\mu$  and the temperature  $T$  allows for a detailed analysis of the lattice formulation at finite density. In the past such an analysis [2] has ruled out the initial incorrect implementation of the chemical potential. Of particular interest here will be the question whether the analytic continuation of the sign function produces divergent  $\mu^2/a^2$  terms. Our study indicates the absence

of such contributions and we find that the  $\mu$  and  $T$  dependence of the energy density is reproduced correctly.

## II. SETUP OF THE CALCULATION

The overlap Dirac operator  $D(\mu)$  for fermions with a chemical potential  $\mu$  is given as

$$\begin{aligned} D(\mu) &= \frac{1}{a} [1 - \gamma_5 \text{sign} H(\mu)] , \\ H(\mu) &= \gamma_5 [1 - aD_W(\mu)] . \end{aligned} \quad (1)$$

The sign function may be defined through the spectral theorem for matrices.  $D_W(\mu)$  denotes the usual Wilson Dirac operator,

$$\begin{aligned} D_W(\mu)_{x,y} &= \mathbb{1} \left[ \frac{3}{a} + \frac{1}{a_4} \right] \delta_{x,y} - \\ &\sum_{j=1}^3 \left[ \frac{\mathbb{1} - \gamma_j}{2a} U_j(x) \delta_{x+\hat{j},y} + \frac{\mathbb{1} + \gamma_j}{2a} U_j(x-\hat{j})^\dagger \delta_{x-\hat{j},y} \right] - \\ &\frac{\mathbb{1} - \gamma_4}{2a_4} U_4(x) e^{\mu a_4} \delta_{x+\hat{4},y} - \frac{\mathbb{1} + \gamma_4}{2a_4} U_4(x-\hat{4})^\dagger e^{-\mu a_4} \delta_{x-\hat{4},y} . \end{aligned} \quad (2)$$

For later use we distinguish between the lattice spacing  $a$  in spatial direction and the temporal lattice constant  $a_4$ . Periodic boundary conditions are used in the spatial directions, while in time direction we apply anti-periodic boundary conditions. The chemical potential  $\mu$  is coupled in the usual exponential form [2].

For vanishing  $\mu$  the Wilson Dirac operator is  $\gamma_5$ -hermitian, i.e.,  $\gamma_5 D_W(0) \gamma_5 = D_W(0)^\dagger$ . This implies that  $H(0)$  is a hermitian matrix. As soon as the chemical potential  $\mu$  is turned on,  $\gamma_5$ -hermiticity no longer holds, and  $H(\mu)$  is a non-hermitian, general matrix. This fact has two important consequences: Firstly, the eigenvalues of  $H(\mu)$  are no longer real and the sign function for a complex number has to be defined in the spectral representation of  $\text{sign} H(\mu)$ . Secondly, the spectral representation has to be formulated using left and right eigenvectors. This latter problem will be dealt with later when we discuss the evaluation of  $\text{sign} H(\mu)$ . For the sign function of a complex number we use the analytic continuation

proposed in [4] and define the sign function through the sign of the real part

$$\text{sign}(x + iy) = \text{sign}(x). \quad (3)$$

The observable we study here is the energy density defined as

$$\begin{aligned} \epsilon(\mu) &= \frac{1}{V} \langle \mathcal{H} \rangle = \frac{1}{V} \frac{\text{Tr}[\mathcal{H} e^{-\beta(\mathcal{H} - \mu\mathcal{N})}]}{Z} = \\ &= -\frac{1}{V} \frac{\partial}{\partial \beta} \ln \text{Tr} \left[ e^{-\beta(\mathcal{H} - \mu\mathcal{N})} \right]_{\beta\mu=c} = -\frac{1}{V} \frac{\partial \ln Z}{\partial \beta} \Big|_{\beta\mu=c}. \end{aligned} \quad (4)$$

Here  $\mathcal{H}$  is the Hamiltonian of the system,  $\mathcal{N}$  denotes the number operator and  $\beta = 1/T$  is the inverse temperature (in our units the Boltzmann constant  $k$  is set to  $k = 1$ ). The derivatives in the second line are taken such that  $\beta\mu = c = \text{const}$ .

The continuum result for the subtracted energy density of free massless fermions reads (see, e.g., [5])

$$\epsilon(\mu) - \epsilon(0) = \frac{\mu^4}{4\pi^2} + \frac{1}{2} \mu^2 T^2. \quad (5)$$

When working on the lattice, the inverse temperature  $\beta$  is given by the lattice extent in 4-direction, i.e.,  $\beta = N_4 a_4$ . Thus the derivative  $\partial/\partial\beta$  in (4) turns into  $N_4^{-1} \partial/\partial a_4$ . The partition function  $Z$  is given by the fermion determinant  $\det D$  which we write as the product over all eigenvalues  $\lambda_n$ . We thus find

$$\begin{aligned} \epsilon(\mu) &= -\frac{1}{VN_4} \frac{\partial \ln \det D}{\partial a_4} \Big|_{a_4\mu=c} = -\frac{1}{VN_4} \frac{\partial \ln \prod_n \lambda_n}{\partial a_4} \Big|_{a_4\mu=c} \\ &= -\frac{1}{VN_4} \sum_n \frac{1}{\lambda_n} \frac{\partial \lambda_n}{\partial a_4} \Big|_{a_4\mu=c}. \end{aligned} \quad (6)$$

### III. EVALUATION OF THE EIGENVALUES

According to (6), for the evaluation of  $\epsilon(\mu)$  the eigenvalues  $\lambda_n$  of the Dirac operator  $D$  have to be computed. This is done in three steps: First we bring the Dirac operator for free fermions to  $4 \times 4$  block-diagonal form, using Fourier transformation. Subsequently the spectral representation is applied to the  $4 \times 4$  blocks of  $H$  to evaluate  $\text{sign } H$ . Finally the eigenvalues of the blocks of  $D$  are computed and by summing over the discrete momenta all eigenvalues are obtained.

Following this strategy, one finds for the Fourier transform  $\hat{H}$  of  $H$ ,

$$\hat{H} = \gamma_5 h_5 + i\gamma_5 \sum_{\nu} \gamma_{\nu} h_{\nu}, \quad (7)$$

with

$$\begin{aligned} h_5 &= 1 - \sum_{j=1}^3 [1 - \cos(ap_j)] - \frac{a}{a_4} [1 - \cos(a_4(p_4 - i\mu))], \\ h_j &= -\sin(ap_j) \quad \text{for } j = 1, 2, 3, \\ h_4 &= -\frac{a}{a_4} \sin(a_4(p_4 - i\mu)). \end{aligned} \quad (8)$$

The spatial momenta are given by  $p_j = 2\pi k_j/aN$ , where  $N$  is the number of lattice points in the spatial directions and  $k_j = 0, 1 \dots N-1$ . The momenta in time-direction are  $p_4 = \pi(2k_4 + 1)/a_4 N_4$ ,  $k_4 = 0, 1 \dots N_4 - 1$ .

The remaining diagonalization of  $\hat{H}$  is similar to the construction of the left- and right-eigenfunctions for the free Dirac operator. One finds that  $\hat{H}$  has two different, doubly degenerate eigenvalues

$$\alpha_1 = \alpha_2 = +s, \quad \alpha_3 = \alpha_4 = -s, \quad s = \sqrt{h^2 + h_5^2}, \quad (9)$$

where  $h^2 = \sum_{\nu} h_{\nu}^2$ . The corresponding left- and right-eigenvectors,  $l_j$  and  $r_j$  are given by

$$\begin{aligned} l_1 &= l_1^{(0)} [\hat{H} + s\mathbf{1}], \quad l_2 = l_2^{(0)} [\hat{H} + s\mathbf{1}], \\ l_3 &= l_3^{(0)} [\hat{H} - s\mathbf{1}], \quad l_4 = l_4^{(0)} [\hat{H} - s\mathbf{1}], \\ r_1 &= [\hat{H} + s\mathbf{1}] r_1^{(0)}, \quad r_2 = [\hat{H} + s\mathbf{1}] r_2^{(0)}, \\ r_3 &= [\hat{H} - s\mathbf{1}] r_3^{(0)}, \quad r_4 = [\hat{H} - s\mathbf{1}] r_4^{(0)}. \end{aligned} \quad (10)$$

The constant spinors  $l_j^{(0)}, r_j^{(0)}$  are ( $T$  is transposition)

$$\begin{aligned} l_1^{(0)} &= r_1^{(0)T} = c(1, 0, 0, 0), \quad l_2^{(0)} = r_2^{(0)T} = c(0, 1, 0, 0), \\ l_3^{(0)} &= r_3^{(0)T} = c(0, 0, 1, 0), \quad l_4^{(0)} = r_4^{(0)T} = c(0, 0, 0, 1). \end{aligned} \quad (11)$$

The constant  $c = (2s(s + h_5))^{-1/2}$  ensures the correct normalization, such that the eigenvectors obey  $l_i r_j = \delta_{ij}$ .

Using these eigenvectors and the spectral theorem we find for  $\text{sign } \hat{H}$  the simple result

$$\text{sign } \hat{H} = \sum_{j=1}^4 \text{sign}(\lambda_j) r_j l_j = \frac{\text{sign}(s)}{s} \hat{H}. \quad (12)$$

Plugging this back into the overlap formula (1) and diagonalizing the remaining  $4 \times 4$  problem one finds two different eigenvalues for the overlap operator at a given momentum,

$$\lambda_{\pm} = \frac{1}{a} \left[ 1 - \frac{\text{sign}(\sqrt{h^2 + h_5^2}) h_5 \pm i\sqrt{h^2}}{\sqrt{h^2 + h_5^2}} \right], \quad (13)$$

where each of the two eigenvalues is twofold degenerate. The momentum dependence enters through the components  $h_{\nu}, h_5$  defined in (8). In the spectral sum (6) the label  $n$  runs over all momenta and the eigenvalues at fixed momentum as given in (13). The necessary derivative with respect to  $a_4$  is straightforward to compute in closed form, and the spectral sum (6) can then be summed numerically. The argument of the sign function cannot become purely imaginary on a finite lattice, and no  $\delta$ -like terms occur. We remark, that after taking the derivative with respect to  $a_4$ , we set  $a = a_4 = 1$ , i.e., all the results we present are in lattice units.

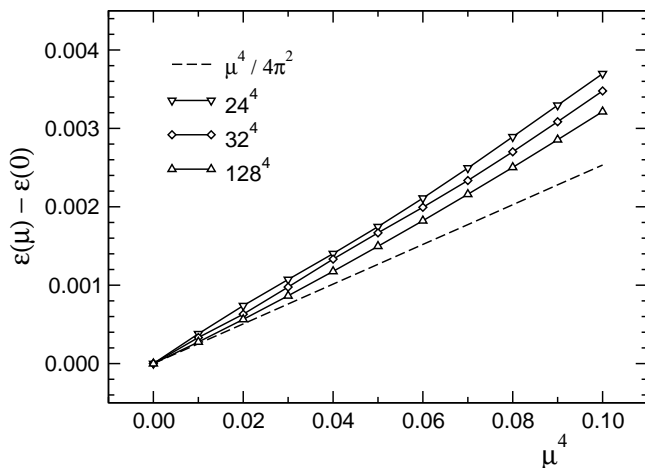


FIG. 1: The energy density  $\epsilon(\mu) - \epsilon(0)$  as a function of  $\mu^4$ . The symbols (connected to guide the eye) are for various lattice sizes, the dashed line is the continuum result.

#### IV. RESULTS

We begin the discussion of our results with Fig. 1, where we show the subtracted energy density  $\epsilon(\mu) - \epsilon(0)$  as a function of  $\mu^4$  for three different lattice volumes. For those lattices all 4 sides have equal length, i.e., in the thermodynamic limit they correspond to zero temperature. Thus, according to (5), we expect the data (symbols in Fig. 1) to approach the continuum form  $\mu^4/4\pi^2$  (dashed line) as the 4-d volume is sent to infinity.

The figure clearly shows that the lattice data are predominantly linear when plotted versus  $\mu^4$  and that for small  $\mu$  they approach the continuum curve when the volume is increased. It is, however, obvious that also on our largest lattice still a discrepancy remains for larger  $\mu$ . In particular one finds a slight curvature upwards, a discretization effect which here, since the lattice spacing is just the inverse lattice extension, is also a finite size effect. Furthermore, for small  $\mu$  one expects to see finite temperature corrections according to (5).

In order to study these finite temperature corrections systematically, we analyzed lattices with short temporal extent, i.e., lattices with non-vanishing temperature. Fig. 2 shows the corresponding results, where we again plot the subtracted energy density as a function of  $\mu^4$ .

The lattice with the shortest temporal extent,  $128^3 \times 8$ , which corresponds to the largest temperature, shows a clear curvature. This curvature is due to the  $T^2\mu^2/2$  term in (5), which appears as a square root when plotted as function of  $\mu^4$ . The effect is visible also for the other lattices, but becomes less pronounced as the temporal extent is increased, i.e., the temperature  $T$  is lowered. In order to study this effect quantitatively, we fit the finite temperature results to the continuum form (5) plus two terms even in  $\mu$  which parameterize the cutoff effects

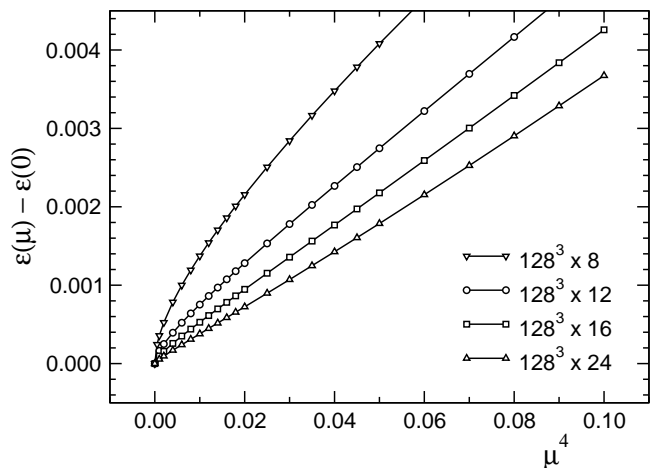


FIG. 2: The energy density  $\epsilon(\mu) - \epsilon(0)$  as a function of  $\mu^4$ , now for finite temperature lattices.

observed in Fig. 1. The fit function is given by

$$c_2 \mu^2 + c_4 \mu^4 + c_6 \mu^6 + c_8 \mu^8. \quad (14)$$

Due to (5) the coefficient of the quadratic term should scale with the temperature such that one expects

$$c_2 \sim T^2/2 = N_4^{-2}/2. \quad (15)$$

The coefficient for the quartic term should be constant,

$$c_4 \sim 1/4\pi^2 = 0.02533. \quad (16)$$

The results of the fit for the data used in Fig. 2, and for the largest lattice of Fig. 1 are given in Table I.

The table shows that with increasing  $N_4$  the two physically significant parameters  $c_2$  and  $c_4$  approach the values expected from the continuum formula (5):  $c_2$  gets closer to  $N_4^{-2}/2$  as listed in the second column, and  $c_4$  approaches  $1/4\pi^2 = 0.02533$ . For the largest finite temperature lattice  $128^3 \times 24$  the discrepancy is down to 9 %

$N_4$	$N_4^{-2}/2$	$c_2$	$c_4$	$c_6$	$c_8$
8	0.007812	0.010125	0.03519	0.010	-0.021
12	0.003472	0.004125	0.03178	0.023	-0.013
16	0.001953	0.002192	0.02803	0.029	-0.015
24	0.000868	0.000947	0.02587	0.025	-0.030
128	0.000030	0.000032	0.02543	0.015	0.016

TABLE I: Results of the fits to the form (14). The spatial volume is always  $128^3$ . The temporal extension  $N_4$  is given in the first column. In the second column we list the corresponding value of  $N_4^{-2}/2$  which is what one expects for the fitting coefficient  $c_2$  in the third column. The coefficient  $c_4$  in the fourth column is expected to approach the constant value  $1/4\pi^2 = 0.02533$ .

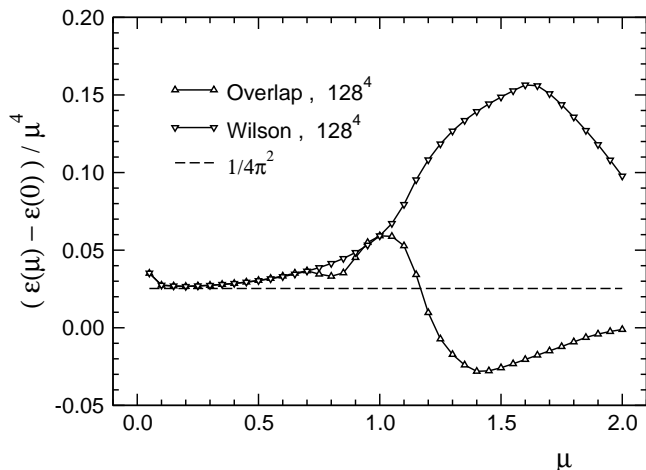


FIG. 3: The ratio  $(\epsilon(\mu) - \epsilon(0))/\mu^4$  as a function of  $\mu$ . We compare the results for overlap to those from Wilson fermions.

for  $c_2$ , and 2 % for  $c_4$ . The larger discrepancy for small  $N_4$  can be understood as a discretization effect, since the temporal lattice spacing  $a_4$  is related to the temporal extension through  $a_4 = 1/N_4$  and thus larger  $N_4$  implies a smaller  $a_4$ . For comparison we also display the fit results for the  $128^4$  lattice, which corresponds to zero temperature. There we find excellent agreement (less than 1% discrepancy) for the parameter  $c_4$ , governing the leading term at  $T = 0$ . The overall picture obtained from the fit results is that overlap fermions with chemical potential reproduce very well both, the  $\mu^4$  term, as well as the finite temperature contribution  $T^2\mu^2/2$ . We conclude that the analytic continuation of the sign function does not introduce lattice artifacts, such as the  $\mu^2/a^2$  term known to be present in a naive implementation of the chemical potential.

In the final step of our analysis we study the discretization effect for larger values of  $\mu$  and compare the results to the data from the standard Wilson operator. In

Fig. 3 we plot the ratio  $(\epsilon(\mu) - \epsilon(0))/\mu^4$  as a function of  $\mu$ . In the continuum at  $T = 0$  this ratio has the value  $1/4\pi^2 = 0.02533$  indicated by the horizontal line. For small  $\mu$ , up to about  $\mu \sim 0.7$ , the Wilson and overlap data fall on top of each other. For very small  $\mu$  both operators show a prominent increase which is a left-over finite temperature effect, which for the ratio  $(\epsilon(\mu) - \epsilon(0))/\mu^4$  shows up as a  $1/\mu^2$  term. In the range between  $\mu = 0.1$  and 0.5 the data are close to the continuum value. Beyond 0.5 the discretization effects kick in and the overlap and Wilson results start to differ. A comparison with the equivalent plot in [6], where the results from various other lattice Dirac operators were presented, shows that the discretization effects of the overlap operator at large  $\mu$  are comparable to other formulations.

## V. SUMMARY

In this article we have analyzed the energy density of the overlap operator at finite chemical potential. Following [4], the sign function in the overlap was implemented through the spectral theorem using the analytic continuation of the sign into the complex plane. The subtracted energy density  $\epsilon(\mu) - \epsilon(0)$  was analyzed for finite and zero temperature lattices. Fits of the data show that the expected continuum behavior is reliably reproduced. No trace of unphysical  $\mu^2/a^2$  terms was found. We conclude that overlap fermions with chemical potential [4] provide both, chiral symmetry and the correct description of fermions at finite density.

**Acknowledgments:** We thank Leonard Fister, Gabriele Jaritz, Christian Lang, Stefan Olejnik, Tilo Wettig, and Florian Wodlei for discussions and checking some of our calculations. This work is supported by the Slovak Science and Technology Assistance Agency under Contract No. APVT-51-005704, and the Austrian Exchange Service ÖAD.

[1] P. H. Ginsparg and K. G. Wilson, Phys. Rev. D 25, 2649 (1982).  
 [2] P. Hasenfratz and F. Karsch, Phys. Lett. B 125, 308 (1983).  
 [3] R. Narayanan and H. Neuberger, Nucl. Phys. B 443, 305 (1995); H. Neuberger, Phys. Lett. B 417, 141 (1998).  
 [4] J. Bloch and T. Wettig, Phys. Rev. Lett. 97, 012003

(2006); J. Bloch and T. Wettig, contribution to Lattice 2006 (hep-lat/0609020).  
 [5] J. Kapusta, Finite temperature field theory, Cambridge University Press, Cambridge (1989).  
 [6] W. Bietenholz and U. J. Wiese, Phys. Lett. B 426, 114 (1998).